ABEL equation for asymmetric emission

F. Pohl

IPP

6/173 July 1978

MAX-PLANCK-INSTITUT FÜR PLASMAPHYSIK

8046 GARCHING BEI MÜNCHEN

MAX-PLANCK-INSTITUT FÜR PLASMAPHYSIK

GARCHING BEI MÜNCHEN

ABEL equation for asymmetric emission

F. Pohl

IPP

6/173 July 1978

Die nachstehende Arbeit wurde im Rahmen des Vertrages zwischen dem Max-Planck-Institut für Plasmaphysik und der Europäischen Atomgemeinschaft über die Zusammenarbeit auf dem Gebiete der Plasmaphysik durchgeführt.

IPP 6/173

F. Pohl

ABEL equation for asymmetric emission

July 1978 (in English)

Abstract

The relation between the emissivity and the test signal is given by ABEL's integral equation. It is nearly always assumed that the emissivity has circular symmetry. This report presents a generalization of ABEL's integral equation for asymmetric emissivities. Both the emissivity and the test signal are expanded in FOURIER series. The generalized ABEL equation is thereby decomposed into a completely separate system of equations for the FOURIER components.

Table of Contents

Introduction

The ABEL integral equation describes the relation between the emissivity F of a domain, which we call "plasma", and the test signal U where the plasma has a circular cross-section and the emissivity F depends only on the distance r from the centre M of the circle (§1).
In this report we investigate what generalizations have to be made to ABEL's integral equation if the emissivity F is not circularly symmetric (eq. (2.2.)). The emissivity F and the test signal U then depend on the angle. If F and U are expanded in FOURIER series, the components satisfy integral equations (2.6) which are partly identical with ABEL's equation and partly of similar construction.
In practice, unfortunately, there are fewer experimental data available than are necessary for proper determination of the emissivity function F. We present the simplest possible interpretation (e.g. at the end of §2) but draw attention to other possibilities (§4, Fig. 12). There are also completely different methods such as /3/.

In § 3 we describe how to determine the plasma centre and radius from the signal functions.
In § 4 we treat the special case of plasmas with quasi-circular symmetry; this primarily concerns elliptical plasmas.

§ 1 Circular symmetry

The plasma cross-section with radius R and centre M is bisected by the line of sight DD' of a detector (Fig. 1).

The detector records all radiation emitted along DD'. With circular symmetry the emissivity F depends only on r, where r denotes the distance of the emitting element ds from the centre M. The detector signal depends only on the position p, where p is the distance of the line of sight from the centre M.

In transparent plasmas it holds that

$$U(p) = \int_{D'}^{D} ds\, F(r) \qquad (1.1)$$

From

$$s = \sqrt{r^2 - p^2} \qquad (1.2)$$

$$ds = \frac{r\, dr}{\sqrt{r^2-p^2}} \qquad (1.3)$$

one gets ABEL's integral equation

$$U(p) = 2 \int_{p}^{R} \frac{dr\, r}{\sqrt{r^2-p^2}}\, F(r) \qquad (1.4)$$

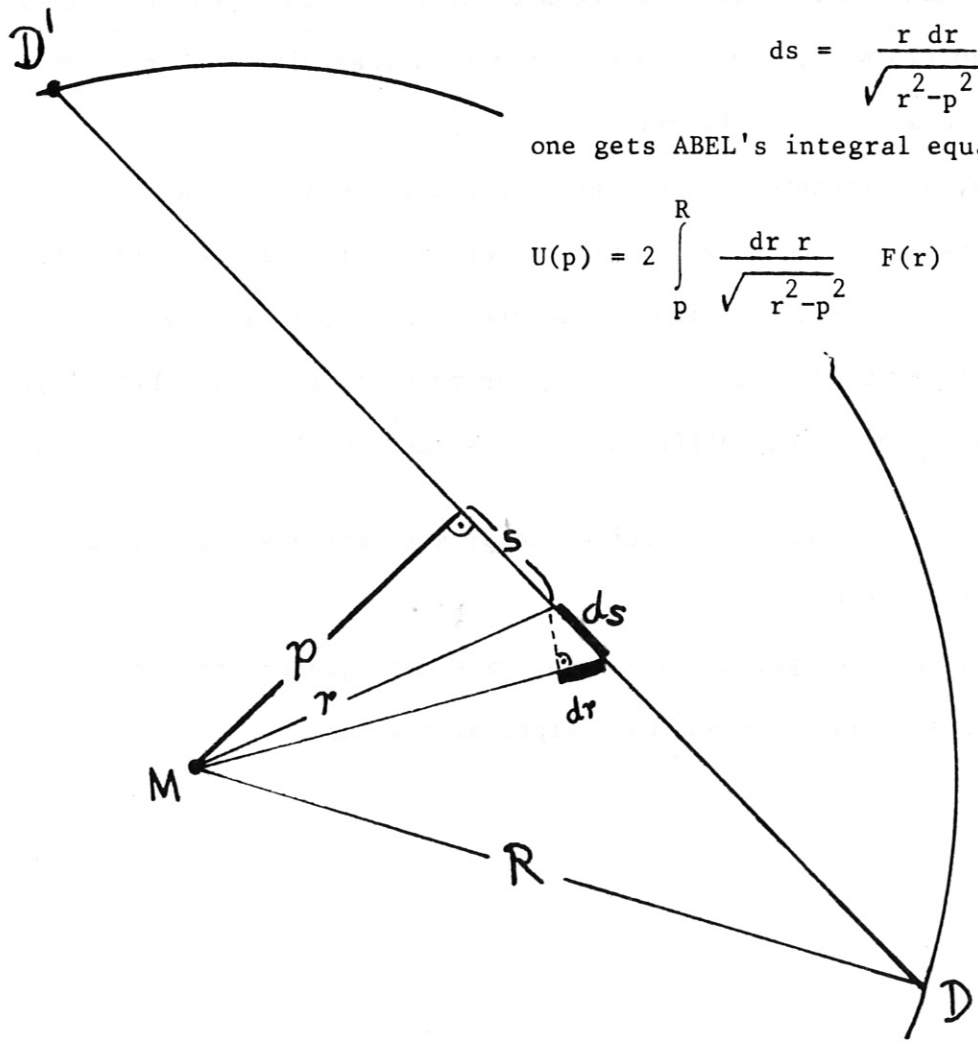

Fig. 1

None of this is new. We have merely repeated these equations here because they are to be generalized later for asymmetric cases. The factor 2 in eq. (1.4) is present because for every r value there are two line elements on DD'; see Fig. 3 in §3.

Below we present a table of ABEL transforms similar to TABLE 1 ABEL TRANSFORMS in /1/, but with a different selection of functions.

Table 1 ABEL transforms (R = 1)

F(r)	$U(p) = 2\int_p^1 \frac{dr\ r}{\sqrt{r^2 - p^2}} F(r)$	a	$\sqrt[2]{1+za}$
1	$2(1-p^2)^{0.5}$	0	2.
$1-r^2$	$\frac{4}{3}(1-p^2)^{1.5}$	1	1.3328 ($\frac{4}{3}$ = 1.3333)
$(1-r^2)^2$	$\frac{16}{15}(1-p^2)^{2.5}$	2	1.0665 ($\frac{16}{15}$ = 1.0666)
$(1-r^2)^3$	$\frac{32}{35}(1-p^2)^{3.5}$	3	0.9142 ($\frac{32}{35}$ = 0.9143)
$\delta(q-r^2)$	$(q-p^2)^{-0.5}$ $\quad q > p^2$		
$(1-r^2)^a$	$\frac{2}{\sqrt[2]{1+za}}(1-p^2)^{a+0.5}$		

Here one has $$z \approx 1.+0.273\,\frac{a+1.}{a+1.17} \quad . \qquad (1.5)$$

In column 4 the amplitude is calculated using the approximation equation (1.5). For $a \gtrsim 3$ the inaccuracy is of the order of 10^{-4}, as numerical tests for $a \leq 17$ have shown.

The inversion: is performed as follows:

Let $$U(p) = (1-p^2)^B \quad . \qquad (1.6)$$

This gives

$$F(r) = \frac{1}{2}\,(1-r^2)^{B-0.5}\,\sqrt{1.+\,(B-0.5)\,\left[\,1.+0.273\,\frac{B+0.5}{B+0.67}\,\right]}\quad .$$

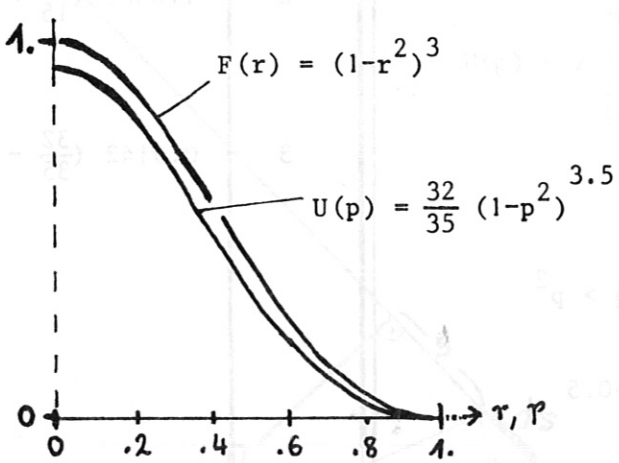

Fig. 2a
(for Table 1, line 4)
Profile with $a \approx 3$
is approximately reproduced
in ABEL transformation

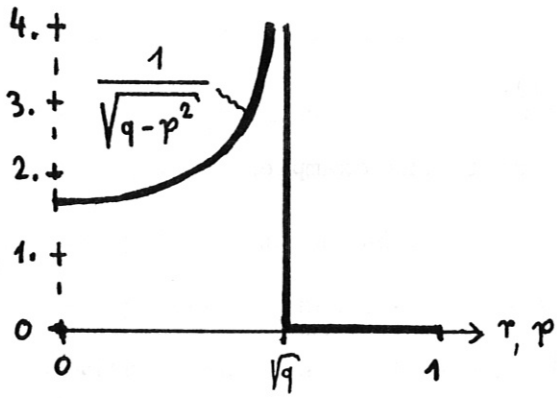

Fig. 2b

(for Table 1, line 5)

$U = 1./\sqrt{q - p^2}$

plotted versus p.

This signal is generated by a ring-shaped emission region of thickness $d \to 0$.

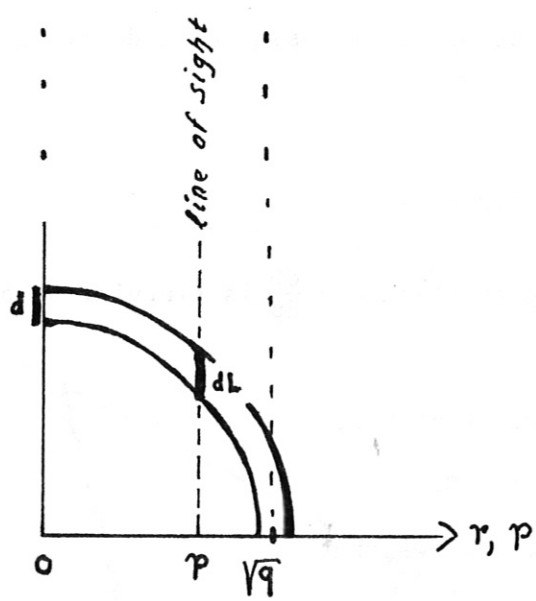

Fig. 2c

Ring-shaped emission region which produces approximately

$U(p) = 1./\sqrt{q-p^2}$

(see Fig. 2b). Line of sight also marked. For the part in the interior of the ring it holds that

$$dL = 2\, d/\sqrt{1-p^2/q}, \quad (1.7)$$

where d = ring thickness.

The factor 2 indicates that the line of sight intersects the ring twice.

It should be noted that the first line of TABLE 1 from /1/ is wrong:

There F(r) is calculated from U(p) according to the formula

$$F(r) = \frac{-1}{\pi} \int_r^1 \frac{dp}{\sqrt{p^2 - r^2}} \frac{dU}{dp}(p) \tag{1.8}$$

(in our report we have $r_o = 1$).

The first line of the table treats the example

$$U(p) = 1. \tag{1.9}$$

It is concluded from it that

$$\frac{dU}{dp} = 0 \text{ and hence } F(r) = 0.$$

This, however, is not true because it is assumed in deriving eq. (1.8) that

$$F(r) = U(p) = 0. \quad \text{for } r,p > 1.$$

Consequently, U(p) is a step function and $\frac{dU}{dp}$ is singular at p = 1.

It is also obvious that:

If a plasma generates a signal U(p) > 0,

its emissivity F must also be > 0.

From eqs. (1.6) and (1.9) it follows that

$$F(r) = 0.315 / \sqrt{1-r^2} \quad . \tag{1.10}$$

The exact solution from eqs. (1.8) and (1.9) is

$$F(r) = \frac{1}{\pi \sqrt{1-r^2}} \quad . \tag{1.11}$$

§2 FOURIER analysis

We now generalize the results from §1 for asymmetric cases.

In §1 R was the plasma radius

and M the plasma centre.

In general, however, we know neither the plasma radius - perhaps there is none - nor the plasma centre. We nevertheless require a reference point M and a radius R. We therefore introduce M and R arbitrarily, but so that the plasma is contained wholly within the circle with radius R and centre M; see Fig. 5.

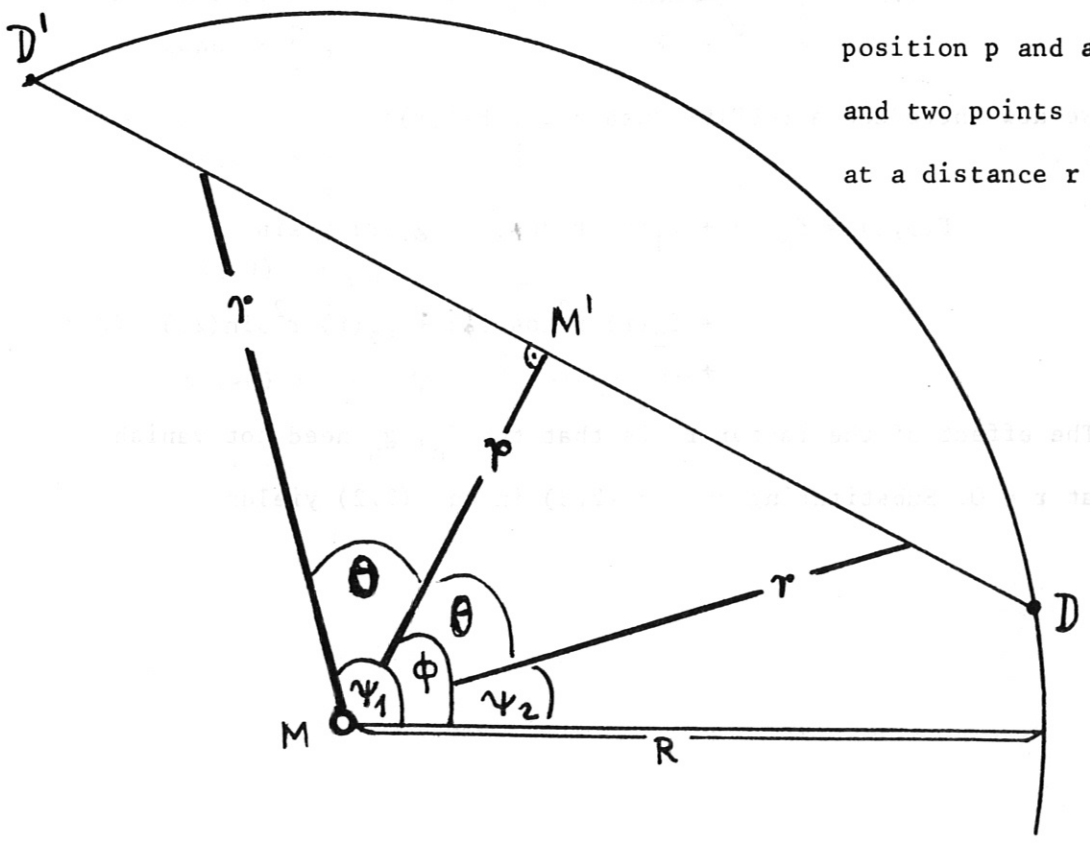

Fig. 3 shows
circle of radius R,
line of sight with
position p and angle ϕ,
and two points
at a distance r from M.

Equation (1.1) is retained.

But F also depends on the azimuth ψ , and U on the angle ϕ :

$$U(\phi,p) = \int_{D'}^{D} ds\ F(\psi(s),\ r(s)).$$

As in §1, we substitute r for s by means of eq. (1.2-3).

From Fig. 3 it can be seen that:

Along D'M' one has $\psi(s) = \psi_1(r) = \phi + \theta$ and (2.1a)

" DM' one has $\psi(s) = \psi_2(r) = \phi - \theta$, (2.1b)

where $\cos\theta = p/r.$ (2.1c)

Equation (1.4) is then generalized as follows:

$$U(\phi,p) = \int_{D'}^{M'} ds\ F(\psi(s),r(s)) + \int_{M'}^{D} ds\ F(\psi(s),r(s)),$$

$$U(\phi,p) = \int_{p}^{R} \frac{dr\ r}{\sqrt{r^2-p^2}} \left[\ F(\psi_1(r),r) + F(\psi_2(r),r)\ \right]. \quad (2.2)$$

We now introduce a FOURIER ansatz for $F(\psi,r)$:

$$F(\psi,r) = f_o(r) + f_1(r)\ r\cos\psi + g_1(r)\ r\sin\psi + f_2(r)\ r^2\cos(2\psi) + g_2(r)\ r^2\sin(2\psi) + \ldots \quad (2.3)$$

The effect of the factor r^n is that the f_n, g_n need not vanish at r = 0. Substituting ansatz (2.3) in eq. (2.2) yields

$$\cos(n\psi_1) + \cos(n\psi_2) = \cos(n(\phi+\theta)) + \cos(n(\phi-\theta))$$
$$= 2\cos(n\theta)\cos(n\phi), \qquad (2.4a)$$

$$\sin(n\psi_1) + \sin(n\psi_2) = 2\cos(n\theta)\sin(n\phi). \qquad (2.4b)$$

One may now ask why there are no terms with $\sin(n\theta)$. The answer is to be found in the peculiarity of the problem: Emissivities are always positive and are thus added; see eq. (2.2). In other problems where there are emissivity "sinks", in addition to "sources" one may also have $\sin(n\theta)$: e.g.

$$\cos(n\psi_1) - \cos(n\psi_2) = 2\sin(n\theta)\sin(n\theta). \qquad (2.4c)$$

The question is what must the FOURIER ansatz for $U(\phi,p)$ look like so that the components for $p \to 0$ neither are singular nor vanish trivially. The answer is to be found in the behaviour of $\cos(n\theta)$:

$$\cos\theta = \frac{p}{r},$$

$$\cos(2\theta) = \frac{1}{r^2}\left[2p^2-r^2\right] \qquad (2.1c)$$

$$\cos(3\theta) = \frac{p}{r^3}\left[4p^2-3r^2\right]$$

$$\cos(4\theta) = \frac{1}{r^4}\left[8p^4-8p^2r^2+r^4\right]$$

....

The odd components have therefore to be multiplied by p,

but not the even components:

The FOURIER ansatz for $U(\phi,p)$ thus reads

$$U(\phi,p) = u_o(p) + u_1(p)\ p\ \cos\phi + v_1(p)\ p\ \sin\phi \qquad (2.5)$$

$$+ u_2(p)\ \cos(2\phi) + v_2(p)\ \sin(2\phi)$$

$$+ u_3(p)\ p\ \cos(3\phi) + v_3(p)\ p\ \sin(3\phi)$$

$$+ \ldots$$

If $U(\phi,p)$ is regarded as defining a function which assigns the value U to every point ϕ,p (in Fig. 3 this is point M') U is singular at p = 0 (in Fig. 3 this is at point M).

We now visualize this in an example:

Let $f_2 = 1.$ $f_{n\neq 2}=0$

$g_n = 0$

$F(\psi,r) = r^2\cos(2\psi).$

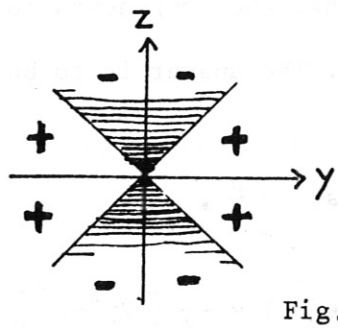

Fig. 4

There are then

two quadrants with positive and

two quadrants with negative

emissivity (see Fig. 4).

A detector with the y axis as line of sight

receives a positive signal $U > 0$;

a detector with the z axis as line of sight

receives a negative signal $U < 0$.

In contrast, it would be expected with an ansatz of type (2.3) that $U(p = 0)$ tends to zero as p^2.

If one defines

$$w = \sqrt{r^2-p^2}$$

and puts eqs. (2.3), (2.5) in eq. (2.2), one obtains by comparing coefficients:

$$u_o(p) = 2 \int \frac{dr\ r}{w}\ f_o(r)\ , \tag{2.6a}$$

$$u_1(p) = 2 \int \frac{dr\ r}{w}\ f_1(r)\ , \tag{2.6b}$$

$$v_1(p) = 2 \int \frac{dr\ r}{w}\ g_1(r)\ , \tag{2.6c}$$

$$u_2(p) = 2 \int \frac{dr\ r}{w}\ f_2(r)\ (2p^2-r^2), \tag{2.6d}$$

$$v_2(p) = 2 \int \frac{dr\ r}{w}\ g_2(r)\ (2p^2-r^2), \tag{2.6e}$$

$$u_3(p) = 2 \int \frac{dr\ r}{w}\ f_3(r)\ (4p^2-3r^2), \tag{2.6f}$$

$$v_3(p) = 2 \int \frac{dr\ r}{w}\ g_3(r)\ (4p^2-3r^2), \tag{2.6g}$$

$$u_4(p) = 2 \int \frac{dr\ r}{w}\ f_4(r)\ (8p^4-8p^2r^2 + r^4), \tag{2.7h}$$

$$v_4(p) = 2 \int \frac{dr\ r}{w}\ g_4(r)\ (8p^4-8p^2r^2 + r^4). \tag{2.7i}$$

.....

All integrals go from p to R. Complete separation is thus achieved with the FOURIER ansatz. Equations (2.6a-c) are identical with eq. (1.4) The other equations differ from it by a factor proportional to $\cos(n\theta)$.

R does not necessarily denote the plasma radius but is the rather arbitrarily selectable radius of the definition domain.

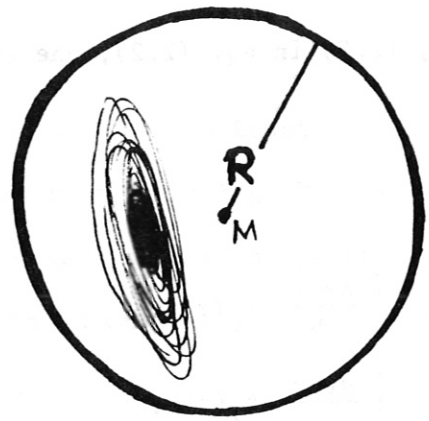

Fig. 5

We now determine the FOURIER components from the given test signals. Let 2N lines of sight be given which all pass the point M at the same distance p; see Fig. 6a,b. The lines of sight differ by the angle ϕ_J. On each line of sight there is a decetor which delivers the test signal

$$U_J = U(\phi_J, p), \qquad J = 1,2...N.$$

It then follows from eq. (2.5) that

$$U_J = u_o + u_1 p \cos\phi_J + v_1 p \sin\phi_J \qquad (2.7)$$

$$+ u_2 \cos(2\phi_J) + v_2 \sin(2\phi_J)$$

$$+ u_3 p \cos(3\phi_J) + ..$$

This makes 2N equations for an infinite number of unknowns. A finite number of test signals thus always admit of an infinite number of interpretations. Examples of this are presented in §4. Here we content ourselves with the "simplest possible interpretation": we set

$$v_{2N} = 0 \ , \tag{2.8}$$

$$v_K = u_K = 0 \quad \text{for} \quad K \geq 2N + 1 \ .$$

Equation (2.7) is then a system of 2N linear equations for the 2N unknowns $u_o, u_1, \ldots u_{2N}, v_2, \ldots v_{2N-1}$.

If the ϕ_J are equidistant: $\phi_J = J \frac{\pi}{N}$ (2.9)

the solution according to ZURMÜHL /2/, §23, eq. (19) is then

$$u_o = \frac{1}{2N} \sum U_J \tag{2.10a}$$

$$u_N = \frac{1}{2N} \sum U_J \, (-1)^J \ , \tag{2.10b}$$

$$\left.\begin{aligned} u_K &= \frac{1}{N} \sum U_J \cos(K\phi_J) \qquad (2.10c) \\ v_K &= \frac{1}{N} \sum U_J \sin(K\phi_J) \qquad (2.10d) \end{aligned}\right\} \quad K = 1,2 \ldots N-1$$

All sums go from J = 1 to J = 2N. The argument p was omitted: $U_J = U_J(p)$.

Finally, it should be mentioned that GOTTARDI in /3/ calculates the asymmetric electron density according to a completely different method which roughly corresponds to the case N = 1 in our scheme.

In Fig.6 we give examples of lines of sight with the same position p for the case N = 3.

With ϕ_J equidistant one observation port is needed for each line of sight (Fig. 6a), while for non-equidistant ϕ_J two lines of sight can be taken through one observation port, so that only N ports are sufficient (Fig. 6b).

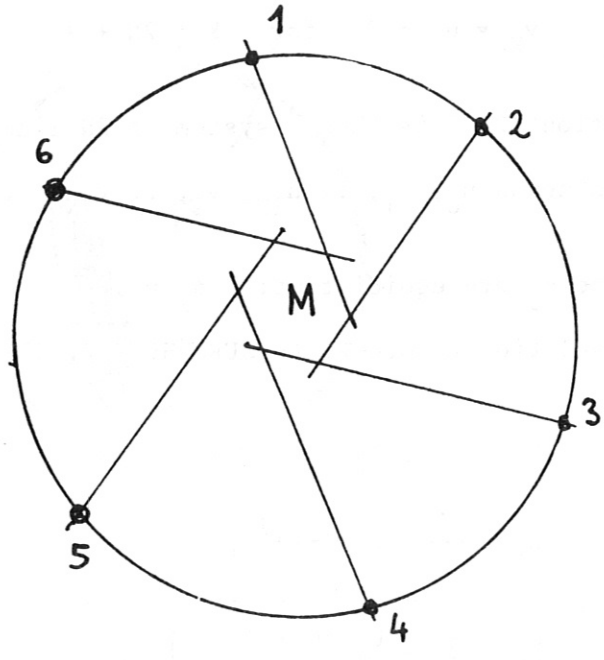

Fig. 6a

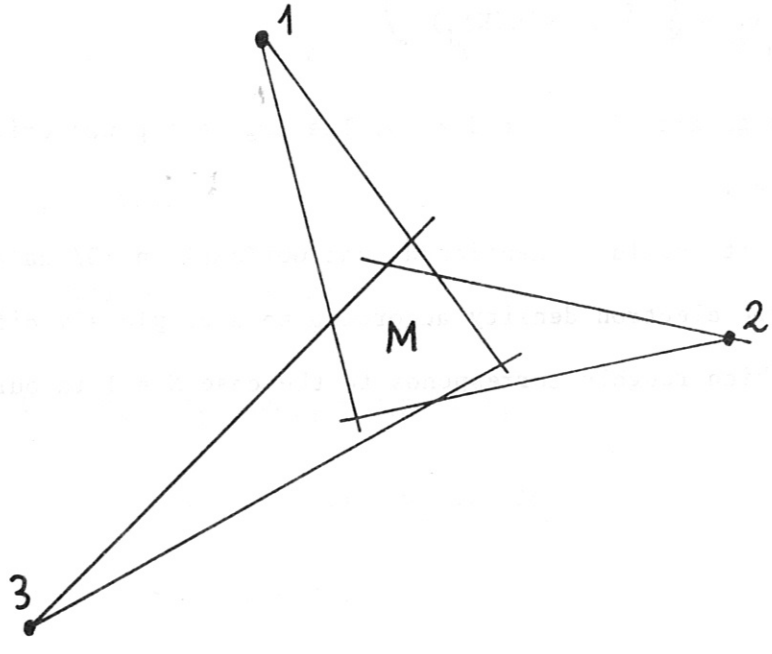

Fig. 6b

§3 Signal functions and plasma centre

To calculate the emissivity $F(\psi,r)$, it is necessary that $U(\phi,p)$ be given, in principle for all points ϕ,p . This, however, is hardly ever the case in practice. If U is not completely given, one has to resort to arbitrary interpretations; see examples at the end of §2 and §4. It seems important to choose the plasma centre properly on the basis of the measured data; this is the subject of this section.

First we describe how the measured data are obtained in principle: Let a few observations ports G_K be given; through each port there pass lines of sight defined by their angle $\hat{\phi}$ to the ordinate. For each line of sight a detector somewhere measures a signal W_K depending on the angle $\hat{\phi}$ of the line of sight. The function $W_K(\hat{\phi})$ is called the "signal function". It holds that

$$W_K(\hat{\phi}) = U(\phi,p). \tag{3.1}$$

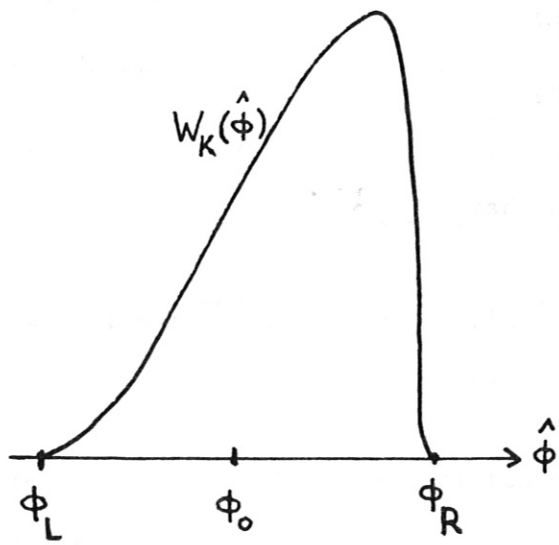

Only when we have determined M will we assign to each $\hat{\phi}$ a pair of values ϕ,p (eqs.(3.4-5).

Fig. 7a
Signal function W_K versus $\hat{\phi}$

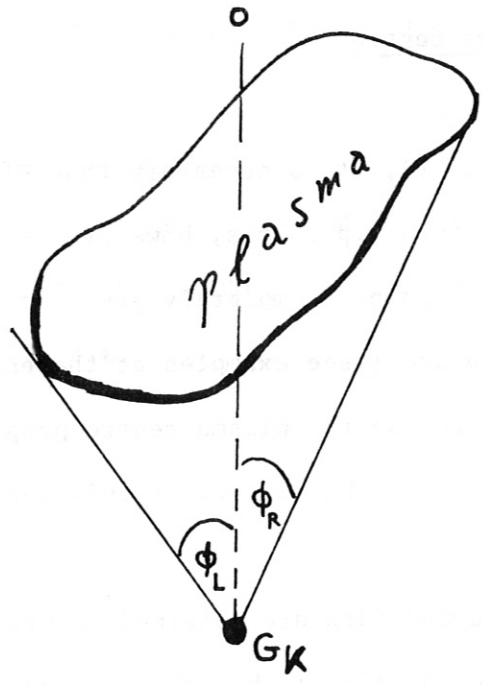

Fig. 7b

Plasma,

observation port G_K,

lines of sight

The observation ports and the respective signal functions are thus experimentally given.

It can be seen from Fig. 7 that there must be two angles $\phi_L^{(K)}$, $\phi_R^{(K)}$ with the property

$$W_K(\hat{\phi}) = 0 \text{ for } \hat{\phi} < \phi_L(K)$$

$$\text{and } \hat{\phi} > \phi_R^{(K)} \quad . \tag{3.2}$$

For the example in Fig. 7 one has

$$\phi_L^{(K)} = -\,40^o,$$

$$\phi_R^{(K)} = +\,25^o \quad .$$

The index (K) indicates that these angles are different for every observation port, i.e. they depend on the port index K.

To determine the plasma centre M we form

$$\phi_o^{(K)} = \frac{1}{2}\left[\ \phi_L^{(K)} + \phi_R^{(K)}\ \right] \tag{3.3}$$

and draw the line of sight with $\phi_o^{(K)}$ for every port G_K. These lines mostly intersect approximately at a point which we use as the plasma centre M (see Fig.8).

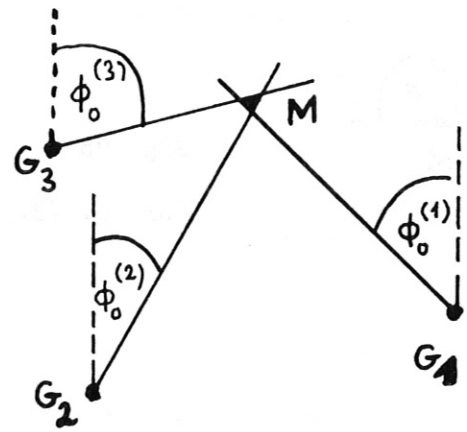

Fig. 8
Three observation ports G_K K = 1, 2, 3 and the lines of sight with the angles $\phi_o^{(K)}$

Once we have calculated M we can replace the variable $\hat{\phi}$ in eq. (3.2) by the position p:

Here a distinction has to be made between two cases:

1.) $\hat{\phi} > \phi_o^{(K)}$,
$$p = g \sin\left[\hat{\phi} - \phi_o^{(K)}\right] \tag{3.4a}$$
$$\phi = -\hat{\phi}, \tag{3.4b}$$

2.) $\hat{\phi} < \phi_o^{(K)}$,
$$p = g \sin\left[\phi_o^{(K)} - \hat{\phi}\right], \tag{3.5a}$$
$$\phi = \pi - \hat{\phi}, \tag{3.5b}$$

where g = distance $G_K M$.

(see Fig. 9)

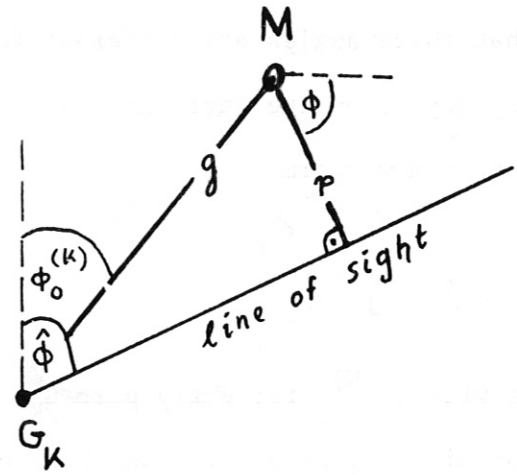

Fig. 9a

For eq. (3.4)

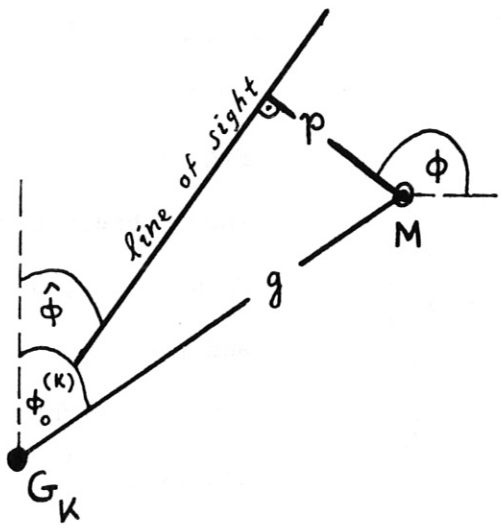

Fig. 9b

For eq. (3.5)

We now define S_K^+ and S_K^- by

$$S_K^+(p) = W_K(\hat{\phi}) \qquad \text{if} \quad \hat{\phi} > \phi_o^{(K)} , \tag{3.6}$$

$$S_K^-(p) = W_K(\hat{\phi}) \qquad \text{if} \quad \phi_o^{(K)} > \hat{\phi} ,$$

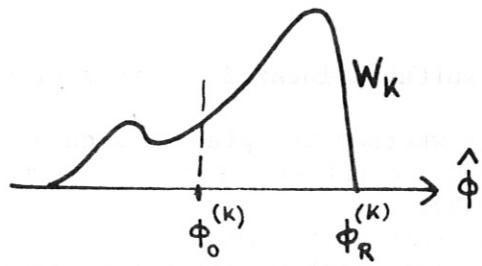

Fig. 10a

W_K versus $\hat{\phi}$

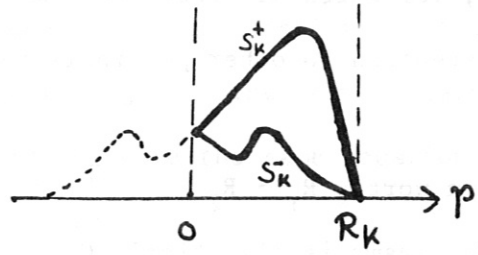

Fig. 10b

S_K^+, S_K^- versus p

where $$R_K = g \sin \left[\phi_R^{(K)} - \phi_o^{(K)} \right] \tag{3.7}$$

= plasma radius, seen from G_K.

§4 Quasi-circular symmetry

We call a plasma "quasi-circularly symmetric" when the signal functions satisfy (see eq. (3.6))

$$S_K^+(p) = S_K^-(p) = S_K(p) \tag{4.1}$$

and $$\frac{S_K(p)}{S_L(p)} = \frac{R_L}{R_K} \quad \text{for two port indices K,L} \tag{4.2}$$

For S_K see eq. (3.6); for R_K see eq. (3.7).

If eqs. (4.1-2) are satisfied, it is mostly possible by linear transformation (the lines of sight thus remaining straight) to achieve that U no longer depends on ϕ , and §1 can be applied. Quasi-circularly symmetric plasmas include such elliptical plasmas as satisfy eq. (4.2), but also, for example, triangular plasmas if

the observation ports are suitably located. It thus often depends on the position of the ports whether the plasma is quasi-circularly symmetric or not (see Fig. 12b).

We now treat a few examples, for which we offer the simplest possible interpretation, but bring attention to other possibilities of interpretation.

Example 1: two observation ports, $R_1 > R_2$

Simplest interpretation: the plasma is elliptical. G_1 is located on one of the principal axes of the ellipse.

Example 1 can be reduced to example 2 (circular symmetry) by linear transformation.

Other interpretations are afforded by dropping the assumption that G_K is located on one of the principal axes (see Fig. 12a).

If there at least three observation ports present, it is possible to determine the position of the principal axes.

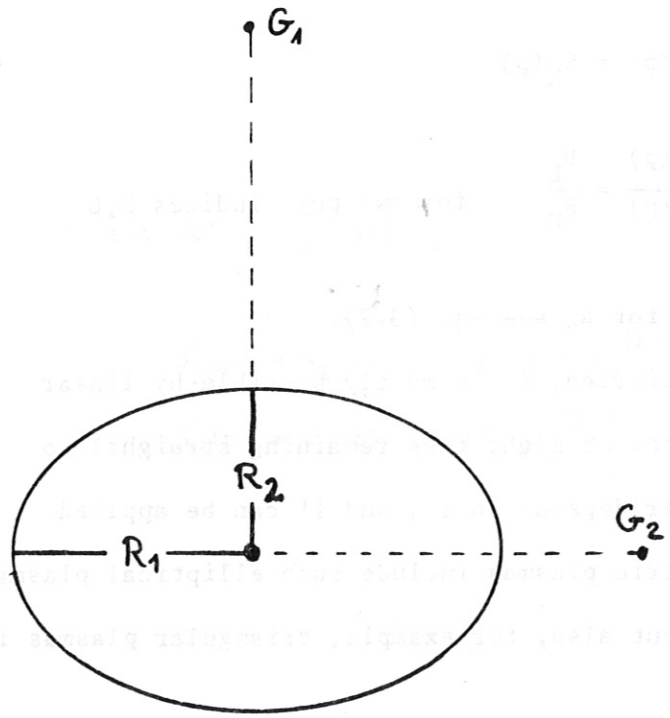

Fig. 11

Simplest possibility for example 1:

G_1 and G_2 are located on the principal axes. From G_1 the plasma radius R_1 appears large, the signal S weak because the lines of sight cover only a short distance R_2 inside the plasma.

Example 2: $S_K(p) = U(p)$ independent of K

Simplest interpretation: the emissivity F is circularly symmetric as in §1. It is obtained by solving the ABEL integral equation (1.4). There are, however, other possibilities of interpretation, two of which are given in Fig. 12. The common feature of these is that the observation ports G_K have the same location relative to the axes of symmetry of the plasma.

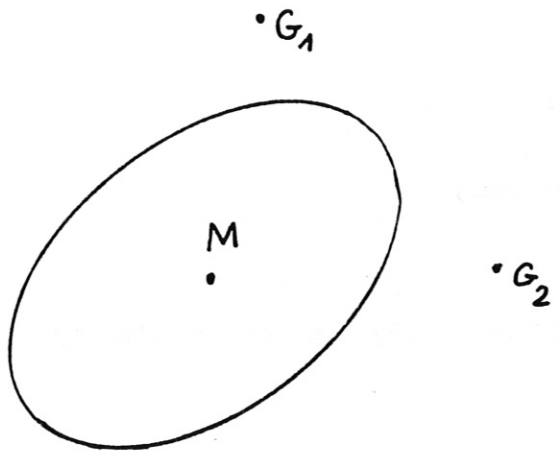

Fig. 12a
Elliptical plasma:
two observation ports, which, however, should be further from the plasma than in the drawing; eq. (4.1) is satisfied for both observation ports.

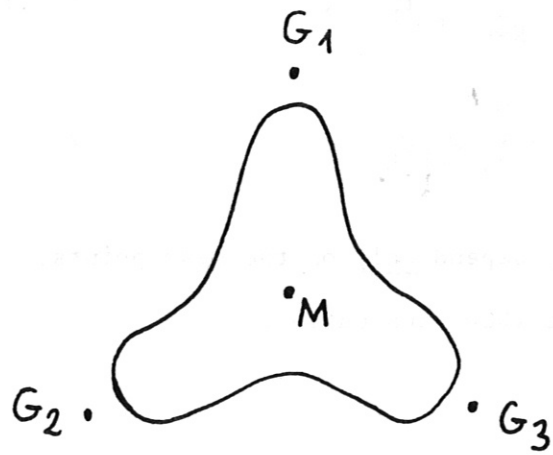

Fig. 12b
Plasma with triangular symmetry:
three observation ports located on the axes of symmetry, otherwise eq. (4.1) would not be valid.

§5 ABEL transformation program

We now solve the ABEL equation for the circularly symmetric case [eq. (1.4); (1.8)] using arbitrary, possibly non-equidistant, mesh points:

$$r_K \ , \ p_L \quad K,L = 1,2, \ldots M \qquad M \leq 11.$$

It must hold that

$$p_K = r_K = R(K) \ , \tag{5.1}$$

$$U_M = U(p_M) = F_M = F(r_M) = 0,$$

i.e. mesh point M must be on the boundary.

Method: Stripwise integration.

The integrands of eqs. (1.4) and (1.8) are approximated by sections of parabolas.

The approximations then read

$$\text{for eq. (1.4)} \qquad U_L = \sum_{K=L}^{M} V_{KL} F_K \ , \tag{5.4}$$

$$\text{for eq. (1.8)} \qquad F_K = \sum_{L=K}^{M} W_{KL} U_L \ . \tag{5.8}$$

The coefficients V_{KL} , W_{KL} depend only on the mesh points. They are computed with the VROUT subroutine.

Use: (if NMAX data records U_L are to be investigated)

1) Mesh point input (R(K), K = 1,M)

2) CALL VROUT (M,R)

3) Dϕ loop

3,1) Data input (U(L), L = 1,M)

3,2) CALL ABEL (F, U, M) gives F from U

3,3) CALL UABEL (F, U_{TEST},M) gives U_{TEST} from F

For testing compare U_{TEST} with U !

Advantage: for large NMAX the computing time required goes almost entirely only on summing according to eqs. (5.4) and (5.8) because the lengthy computations of W_{KL} and V_{KL} are done separately in VROUT subroutine.

```
      $SOURCE
 1          SUBROUTINE  VROUT ( M, R)
 2          DIMENSION       D(11) ,G(11) ,Q(11) ,R(11) ,WD(11)
 3          COMMON /UAB/        V(11,11) ,W(11,11)
 4          DO 1        K=1,M
 5                Q(K) = R(K)**2
 6          DO 1        L=1,M
 7               V(K,L) = 0.
 8        1      W(K,L) = 0.
 9                  M1 = M - 1
10          DO 2        K=1,M1
11        2       D(K) = Q(K+1) - Q(K)
12          DO 5        L=1,M1
13                    L1 = L + 1
14                  G(L) = 0.
15                 WD(L) = 0.
16          DO 3        K=L1,M
17                WD(K) = 2.* SQRT( Q(K) - Q(L))
18        3        G(K) = 0.333333 * WD(K) *(2.* Q(L) + Q(K))
19               W(L,L) = 0.31831*(WD(L+1) -WD(L)) / D(L)
20               W(L,M) = 0.31831*(WD(M-1) -WD(M)) / D(M-1)
21               V(L,L) = (Q(L+1)*(WD(L+1) -WD(L)) +G(L) -G(L+1))/ D(L)
22               V(M,L) = (Q(M-1)*(WD(M-1) -WD(M)) +G(M) -G(M-1))/ D(M1)
23          DO 4        K=L1,M1
24          IF ( K. GE. M)       GO TO 5
25               W(L,K) = 0.31831*( (WD(K+1)-WD(K))/D(K)
          1                        + (WD(K-1)-WD(K))/D(K-1))
26        4      V(K,L) = (Q(K+1)*(WD(K+1)-WD(K))+G(K) -G(K+1)) / D(K)
          1             + (Q(K-1)*(WD(K-1)-WD(K))+G(K) -G(K-1)) /D(K-1)
27        5 CONTINUE
28          RETURN
29          END

30          SUBROUTINE UABEL ( F, U, M)
31          DIMENSION   F(11) , U(11)
32          COMMON /UAB/        V(11,11) ,W(11,11)
33                F(M) = 0.
34                U(M) = 0.
35                  M1 = M - 1
36          DO 3        L=1,M1
37                    SU = 0.
38          DO 1        K=L,M1
39        1             SU = SU + V(K,L) * F(K)
40        3         U(L) = SU
41          RETURN
42          END

43          SUBROUTINE  ABEL ( F, U, M)
44          DIMENSION   F(11) , U(11)
45          COMMON /UAB/        V(11,11) ,W(11,11)
46                F(M) = 0.
47                U(M) = 0.
48                  M1 = M - 1
49          DO 3        K=1,M1
50                    SU = 0.
51          DO 1        L=K,M1
52        1             SU = SU + W(K,L) * U(L)
53        3         F(K) = SU
54          RETURN
55          END
```

References

/1/ NASA TN D-5677 Feb. 1977

/2/ R. ZURMÜHL
Praktische Mathematik
für Ingenieure und Physiker
Springer Verlag Berlin, Heidelberg, N.York
1965

/3/ N. GOTTARDI IPP III/39 Dez. 1977